Design and Development of a Fixed Wing Unmanned Aerial Vehicle (UAV) Prototype for Crop Spraying

Guruprasad M. Godbole[#1], Kalyani K. Bhadekar[#2], Sahib Bir Singh[#3], Sai S. Aranke[#4]
[#] *Department of Mechanical Engineering, Sinhgad College of Engineering, Pune, India*

***Abstract*— The aim of this paper is to design and develop a fixed wing Unmanned Aerial Vehicle (UAV) prototype for crop spraying. The need to implement UAVs for crop spraying, literature review, design methodology, fabrication and testing of the prototype have been presented. Design methodologies of fixed wing UAVs, agricultural applications of UAVs as well as various methods of control of UAVs have been studied and presented in the literature review. The design methodology for this project has been elaborated in the third section. The mission requirements and the conceptual design have been elaborated first, followed by the preliminary design, which involves airfoil selection, aerodynamic design of wing and selection of the components of the propulsion system. Analysis in XFLR5 was performed for airfoil selection, wing design and tail design. The detail design expounds the structural design and analysis of wing and tail, the fuselage configuration and the spraying system to be implemented. The fabrication and testing of the prototype, its observations and results have been discussed in the last two sections.**

***Keywords*—UAV, fixed wing, crop spraying, design, analysis, fabrication, testing**

I. INTRODUCTION

The manned aircrafts suffered from drawbacks such as limits on range and endurance, large risk and loss of life, probability of being captured as well as high production and operation costs. Unmanned Aerial Vehicles (UAVs) helped overcome most of the drawbacks of manned aircrafts which led to the emergence of UAVs and further research and development. A UAV is an aircraft with no pilot on board. UAVs are controlled via a remote-control device or fly autonomously with pre-programming. UAVs have a very broad scope of applications which includes reconnaissance, combat, research and development, civil and commercial [1]. There are applications like crop spraying [2], agricultural surveillance and meteorological data acquisition [3] where employing human effort is unsafe, vexatious or simply not required altogether.

However, the application of UAVs in precision agriculture is relatively unexplored and has tremendous potential for increasing the crop yield in an economical manner. The agricultural uses of UAVs are more focused on low altitude operations over small fields. For example, crop spraying is being currently implemented in Japan where the average the field size 19000 m^2 and 40% of the rice fields are sprayed using drones [4].

The World Health Organization (WHO) estimates there are more than 1 million pesticide cases in every year. In that, more than one lakh deaths occur each year, especially in developing countries due to the pesticides sprayed by human beings [5]. Considering the average field size in India (which is less than 10000 m^2) crop spraying using UAVs can be implemented on a larger scale in India too. This project aims to provide a safer alternative way of spraying pesticides in order to address the issue of the large number of deaths occurring due to the pesticides sprayed by human beings.

The UAVs are however, not without their limitations. Experiences indicate that current UAV technologies have a number of limitations for practical implementation in agriculture such as cost, payload, susceptibility to animal or bird attacks, lack of standard protocols for UAV development, sensitivity of communication, necessity of a skilled operator and possibility of mechanical and electrical failure.

Section II describes the literature review encompassing various aspects of the project. Section III describes the design methodology that was followed during the course of the project. Section IV details the fabrication and assembly of the prototype. Section V discusses the testing, observations and results obtained through the testing of the UAV prototype.

II. LITERATURE REVIEW

Kontogiannis and Ekaterinaris [6] have performed a complete study of a small-size light UAV, which includes design, construction and in-flight testing. The preliminary design included aerodynamic performance and stability analysis. CFD analysis was performed to evaluate aerodynamic characteristics and efficiency of the airfoil, the wing and the full configuration; and to serve as basis for the optimization process. With further aerodynamic improvements using CFD analysis and structural optimization, it is expected that a similar design could fly using solar power.

Panagiotou *et al.* [7] have explained the aerodynamic design procedure of a Medium-Altitude-Long-Endurance (MALE) Unmanned Aerial Vehicle (UAV), by dividing it into conceptual and preliminary design stages. The study focuses on the aerodynamic aspects of the Hellenic Civil Unmanned Aerial Vehicle (HCUAV) project which involves design and construction of a prototype to perform civil operations in Greece.

Giles and Billing [2] have assessed the performance of a commercially manufactured, remote controlled petrol-powered helicopter After spraying, the leaves were sampled for chemical analysis to quantify the deposition. It was found that UAVs can be successfully deployed for specialty crop spraying conditions as excellent spray rates were achieved considering the limitations of the aircraft.

Huang *et al.* [8] have presented an analysis of research depicting the development of UAV technology for management of agricultural production. Mainly, UAVs for aerial applications over agricultural land (e.g. crop spraying using low volume system) are studied. Limitations of current UAVs like technical decisions, cost, payload, operation and reliability as well as ways to overcome have been discussed at length.

Ahmed *et al.* [9] have developed a state space model for both linear and lateral dynamics of a small unmanned aerial vehicle (SUAV), for designing the autopilot with various phases of flight.

Cappello *et al.* [10] have presented a multi-sensor data fusion technique which uses various sensors and an extended kalman filter to fuse the data of the sensors to provide correct state estimate of the UAV.

III. Design and Analysis

The design methodology is based on the traditional methods described in [11] and [12]. The methodology first involves selecting a mission profile and defining a set of requirements, i.e. the operational requirements such as flight velocities, endurance and range, as per the application. The first phase of design is conceptual design, which is followed by preliminary design and finally, detail design. Fabrication takes place after the detail design.

Since the application of this project is crop spraying, it was important to decide the crop under consideration. Crops such as rice, wheat, grapes and mango were considered for the application, from which grapes were found to be the most feasible. According to the data obtained from [13], a field size of 118x75 square meters was considered for the application and the spraying pattern illustrated in Fig.1 was proposed.

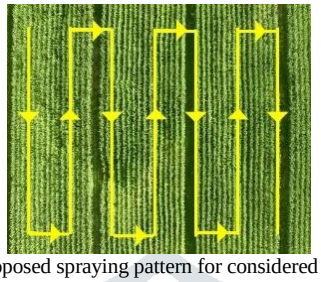

Fig.1. Proposed spraying pattern for considered field size

TABLE I.
MISSION REQUIREMENTS

Parameter	Value
Gross take-off weight	3 kg
Stall velocity (*Vstall*)	7-9 m/s
Cruise velocity (*Vcruise*)	11-13 m/s
Take-off velocity (*Vtake-off*)	8.4-10.8 m/s

The primary objectives in the preliminary design phase were airfoil selection and aerodynamic design of the wing, considering the mission requirements. Additionally, power system calculations and a control system case study were also performed.

In order to select the airfoil, analysis was performed using XFLR5, which is a tool for analysis of airfoils, wings and planes operating at low Reynolds numbers.

Considering the above requirements, a number of airfoils were analyzed for Reynolds numbers ranging from 0 to 900,000 in XFLR5, for angle of attack (α) varying from -5° to 15°. After the initial analysis, the airfoils MVA 227, Selig 1210 and Selig 1223 were found to be the most suitable. Therefore, the above mentioned airfoils were considered for the final airfoil selection.

TABLE II.
SELECTION OF FINAL AIRFOIL USING WEIGHTED POINT METHOD

Criteria	Weight (%)	MVA 227	Selig 1210	Selig 1223
C_l vs. α	20	60	70	80
C_d vs. α	20	70	50	80
(C_l/C_d) vs. α	30	80	70	50
Strength	10	70	50	50
Manufacturability	20	60	40	40
Total	100	69	58	60

From TABLE II, it can be observed that MVA 227 is the airfoil with the most points. Considering all the criteria, MVA 227 was the airfoil selected.

Considering the mission requirements, as well as important factors such as simplicity, manufacturability and cost, it was found that a high wing with a rectangular planform was best suited for the need [14].

The next step was the determination of the optimum values of two factors, namely Wing Loading (*W/S*) and Thrust-to-Weight ratio (*T/W*). For this purpose, a constraint diagram was plotted as shown in Fig.2, with the help of equations relating the two factors for cruise and take-off conditions [15]. The condition for stall dictates the maximum limit for the value of (*W/S*), was found to be 63 N/m^2.

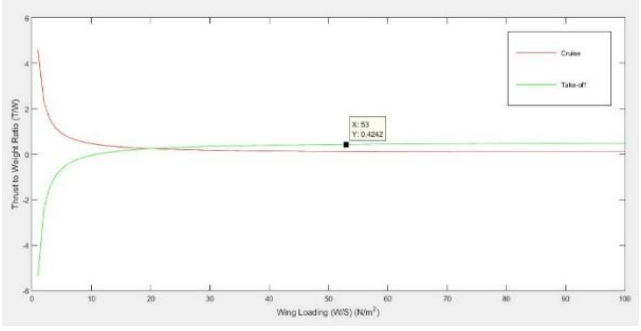

Fig.2. Constraint Diagram

TABLE III.
DETAILS OF AERODYNAMIC DESIGN OF WING

Parameter	Value
Wing span (*b*)	1.6764 m
Chord length (*c*)	0.3353 m
Wing planform area (*S*)	0.561 m^2
Aspect Ratio (*AR*)	5.00
Angle of attack (α)	0°
Wing Loading (*W/S*)	53 N/m^2

The fixed-lift analysis was conducted in XFLR5 in order to check whether the thrust obtained from the (*T/W*) value at a particular value of (*W/S*) for cruise condition, was greater than the drag force experienced. Next, the fixed-velocity analysis was conducted in order to examine whether the thrust obtained from the (*T/W*) value at a particular value of (*W/S*) for take-off condition was sufficient to overcome the drag force. Through an iterative process, it was found that (*W/S*) = 53 N/m^2 was the most optimum as per the requirements. It was also observed that the cruise velocity was obtained at α=0°. The values of (*T/W*) at (*W/S*) = 53 N/m^2 were found to be 0.4242 for take-off condition and 0.1171 for cruise condition.

A. Propulsion

An electric power source was picked to power the propeller owing to its easy installation and use, cost-effectiveness and because it is eco-friendly in nature compared to an engine. A LiPo battery of 2200 mAh was chosen to power a brushless motor of 840 kV. A propeller of a configuration of 11x5.5E was mounted on the motor shaft. An Electronic Speed Controller (ESC) of a current rating of 40A was selected to control the speed of the motor in correlation with the power supplied by the battery.

B. Structural Design of Wing

The main function of the wing is to generate adequate lift force or simply lift. However, the wing also experiences the drag force or drag and nose-down pitching moment. While a wing designer aims to maximize the lift, the drag and pitching moment must be minimized [14].
The curve of lift coefficient along the span of the wing is elliptical in shape. For simplicity in calculations, the force acting along the span was converted to two uniformly varying loads at the ends of the wing and uniformly distributed load at the centre of the wing as shown in Fig.3. The lifting force acting at these points was calculated and multiplied by a factor of 3 to account for the approximation and the safety of the structure.

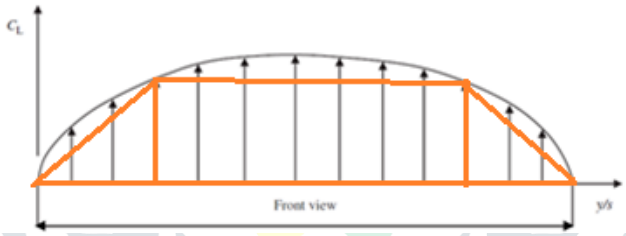

Fig.3. Elliptic wing loading

The wing was constructed using 16 ribs made of 5mm thick balsa wood sheets and 2 aluminium spars. Through an iterative process, the positioning of the two aluminium spars was found to be optimum at 10% and 50% of the chord length of the airfoil. For support and strength, the leading and trailing edges are masked using 1 mm thick balsa sheet.

TABLE IV.
STRESS AND DEFORMATION SUMMARY FOR WING

	Equivalent Stress (MPa)	Total Deformation (mm)
Minimum	1.7152e-006	0
Maximum	21.7	0.27183

Fig.4 shows the total deformation and equivalent stress acting on the wing. It was concluded that the structure was safe as it could sustain 3 times the calculated load without substantial deformation.
The control surfaces of the wing, i.e. the ailerons were sized using empirical values obtained from [14]. The combined span of the ailerons was selected to be 0.25 times the wingspan, and the span of each aileron was in turn half of the combined span of the ailerons. A chord length of 0.2 times the wing chord was found to be suitable for the ailerons.
Aluminium tubes of 8 mm diameter and 1 mm thickness were used as spars. Fig.4 shows the total deformation and equivalent stress acting on the spars.

TABLE V.
STRESS AND DEFORMATION OF SPARS

	Equivalent Stress (MPa)	Total Deformation (mm)
Minimum	1.9237e-12	0
Maximum	1.7242e-3	0.4089e-6

From TABLE V, it is seen that the maximum deformation and stress, that acts at the end of the spar, is negligible. Therefore, the design of the spar is safe at the maximum loading condition.

Fig.4. Total deformation and equivalent stress for wing

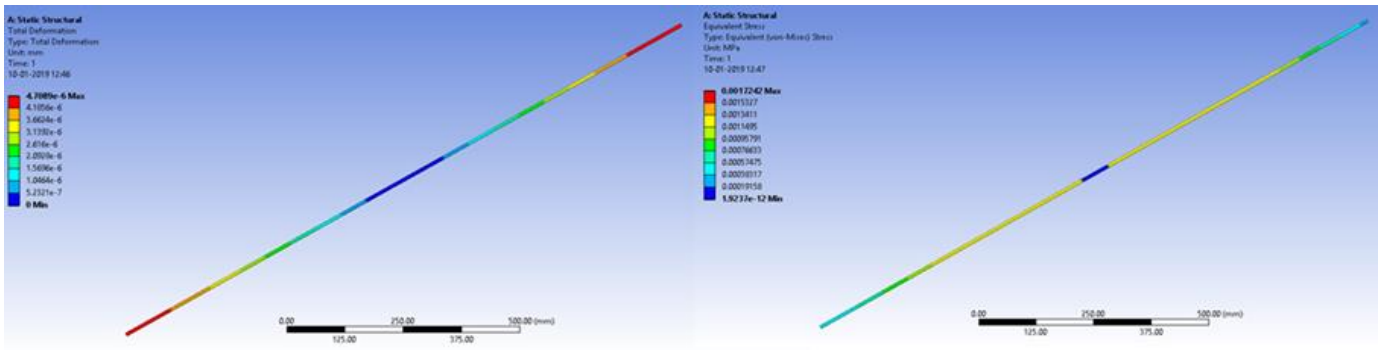

Fig.5. Total deformation and equivalent stress for spar

C. Tail Design

The next appropriate step after wing design is design of tail. The tail was designed through an iterative

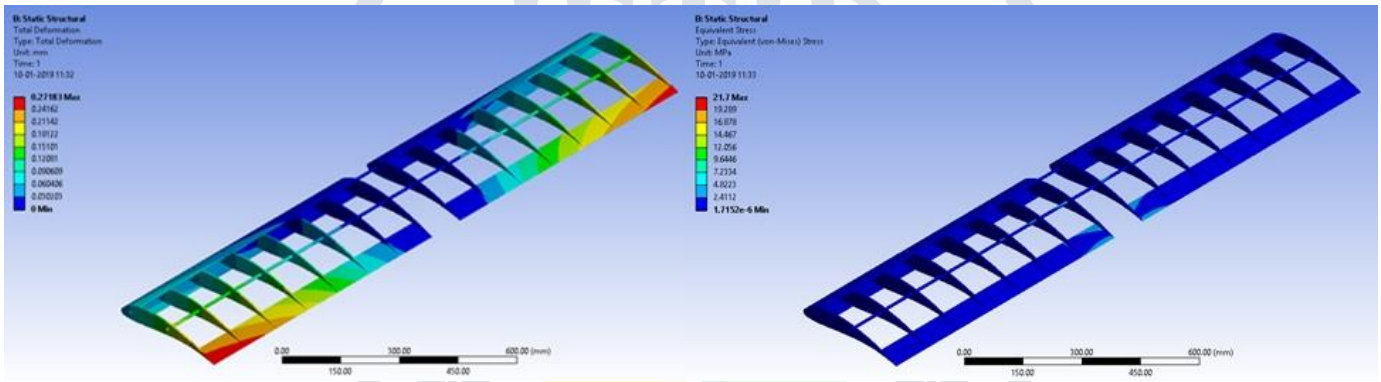

process by selecting suitable values of tail volume coefficients from empirical data available in [11] and considering various values of the tail moment arm. After obtaining the two parameters mentioned above, the area of the horizontal and vertical tail was estimated by using (1) & (2) respectively [12].

$$V_H = \frac{l_H}{C} * \frac{S_H}{S} \quad (1)$$

$$V_V = \frac{l_V}{b} * \frac{S_V}{S} \quad (2)$$

where,
V_H and V_V = Horizontal tail volume ratio and vertical tail volume ratio respectively
l_H and l_V = Horizontal and vertical tail moment arm respectively (m)
S_H and S_V = Planform area of horizontal and vertical tail respectively (m^2)
C = Mean aerodynamic chord of the wing (m)
b = Wingspan (m)
S = Wing planform area (m^2)

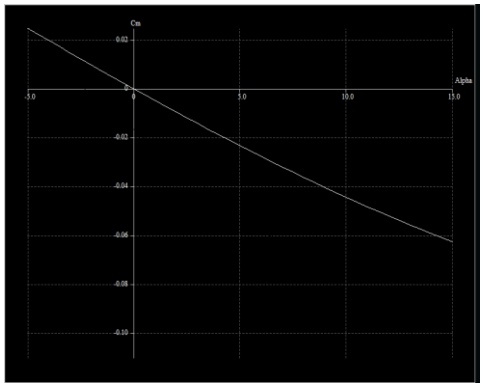

Fig.6. Pitching moment coefficient (C_m) vs α graph for horizontal tail

The dimensions of horizontal tail were obtained for different values of horizontal tail volume coefficient (ranging from 0.5 to 0.7), tail moment arm [ranging from 0.91 m to 1.82 m (3 ft to 6 ft)] and a suitable aspect ratio (usually 0.5 to 0.6 times the aspect ratio of the wing). Subsequently, the various configurations were analysed in XFLR5 to check for longitudinal static stability and the graph of pitching moment coefficient (C_m) vs angle of attack (α) was obtained. For an aircraft to have static stability, the graph must have a negative gradient. From Fig.6, it can be observed that the C_m vs α graph has a negative gradient and it passes through the origin, since the angle of attack is 0°.

It was found that the optimum configuration was obtained for horizontal tail volume coefficient 0.61 and tail moment arm of 1.068 m (3.5 ft), having a planform area 0.108 m^2. The vertical tail dimensions were also estimated in a similar way. Since the vertical tail does not contribute to the longitudinal stability, it was not required to analyse the same in XFLR5. The value of vertical tail volume coefficient selected was 0.04 and the area of the vertical tail obtained was 0.0308 m.

The control surfaces of the horizontal and the vertical tail, i.e. the elevator and rudder respectively were sized using empirical values obtained from [14]. The span of the elevator was chosen to be the same as that of the horizontal tail. A chord length of 0.3 times the horizontal tail chord was found to be suitable for the elevator. Similarly, the vertical span of the rudder was chosen to be of the same length as that of the vertical tail, and the chord to be 0.3 times that of the chord of the vertical tail.

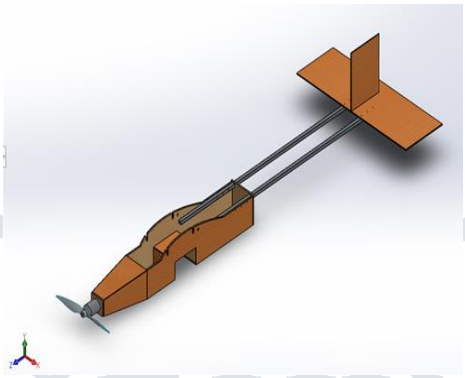

Fig.7. Twin boom configuration for tail

Considering the strength requirement of the tail, 5 mm thick balsa wood along with 1.5 mm thick aeroply was used for the tail. A twin-boom configuration was found to be the optimum configuration for our UAV design as it increases UAV's rigidity and strength. Fig.7 shows the twin boom configuration proposed for our UAV design. Square aluminium tubes with side 12.5 mm and 1 mm thickness were selected considering their strength, weight and availability. Fig.8 shows the total deformation and equivalent stress acting on the boom. It was concluded that the structure was safe as it could sustain 3 times the calculated load without substantial deformation.

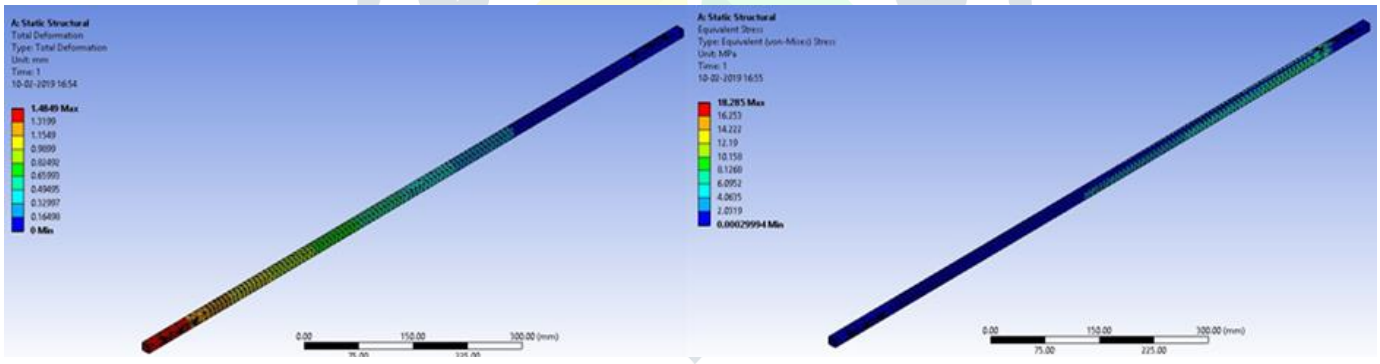

Fig.8. Total deformation and equivalent stress for boom

TABLE VI.
STRESS AND DEFORMATION SUMMARY FOR BOOM

	Equivalent Stress (MPa)	**Total Deformation (mm)**
Minimum	2.9941e-4	0
Maximum	18.285	1.4849

D. Fuselage Configuration

The fuselage, or the body of the UAV, holds all the pieces of the UAV together. Its main function is to support the load from the wing, tail, motor and the payload. A box type rectangular configuration of fuselage was found to be the best choice for our application. The fuselage was constructed using 5mm thick balsa wood along with 1.5mm thick aeroply.

As seen from Fig.9, the upper curve of the airfoil selected for wing is used for the walls of the fuselage along with two slots for the spars of the wing. This technique ensures the desired high wing configuration and allows easy mounting and dismounting of the wing. The front section of the fuselage, or the 'nose' is specifically tapered to support the motor and propeller and reduce

drag. The motor along with the propeller is mounted on the nose of the fuselage using a motor mount which blocks any vibration or movement that can potentially affect the propeller's performance.

As illustrated in Fig.10, a rectangular slot is made in the fuselage to house the container which carries the payload. A pipe is drawn from the lid of the container and connected to a spraying head. The spraying head is fitted outside the fuselage between the rear landing gear and the container. The electronics which drive the spraying system are placed on a wooden base inside the fuselage on top of the container. The battery and the Electronic Speed Controller (ESC) are placed in the front section of the fuselage in order to achieve the desired location of centre of gravity, by ensuring proper distribution of weight. A conventional tricycle landing gear was used for our UAV. It consists of a single wheel near the nose of the fuselage and two wheels at the back of the fuselage. This configuration allows for easy manoeuvrability of the UAV and provides stability to the UAV. The height of the landing gear was decided considering the height of the container.

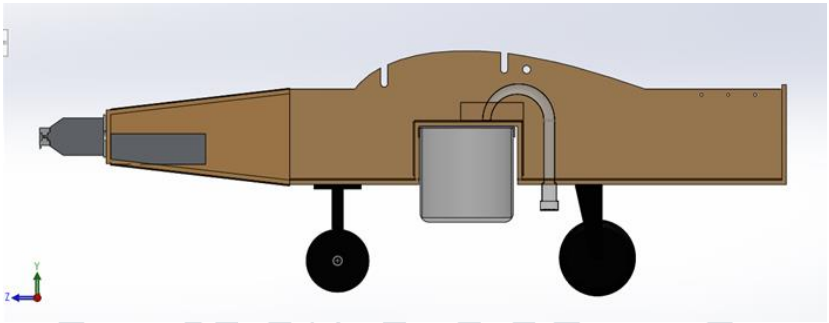

Fig.9. Section of side view of the fuselage

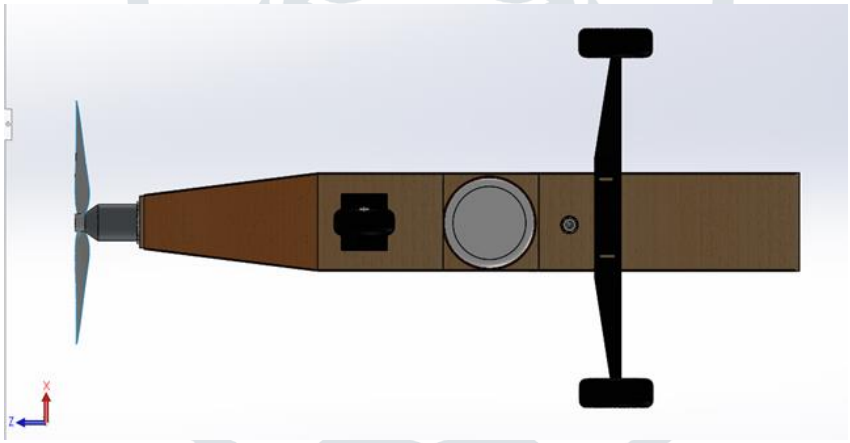

Fig.10. Placement of landing gear

E. Spraying Mechanism

The spraying mechanism consists of the following components: cylindrical container of diameter 9.5cm and height 10 cm, flexible pipe of 5 mm diameter, submersible pump, Arduino Uno microcontroller, L293d motor driver, Ultrasonic level sensor and 12V, 9V batteries.

According to the application requirements, a submersible pump of 100 litres/hour discharge is selected which delivers pesticide for the given field size in two flight rounds. The pump is placed at the base of the container and the pesticide is carried by a flexible pipe to the spraying head. The pump is controlled by Arduino Uno microcontroller which is based on the microchip ATmega328P. An ultrasonic level sensor attached to the lid of the container senses the level of pesticide in the container and provides a closed loop feedback control. The interfacing diagram of the microcontroller with the sensor and pump is shown in Fig.11. The submersible pump is connected to the Arduino Uno microcontroller via a L293d motor driver circuit which has both 12V as well as 5V pins for connecting the pump and microcontroller respectively. The microcontroller is powered by a 9V battery. As soon as the level of pesticide drops below the delivery of the pump, the microcontroller switches off the pump.

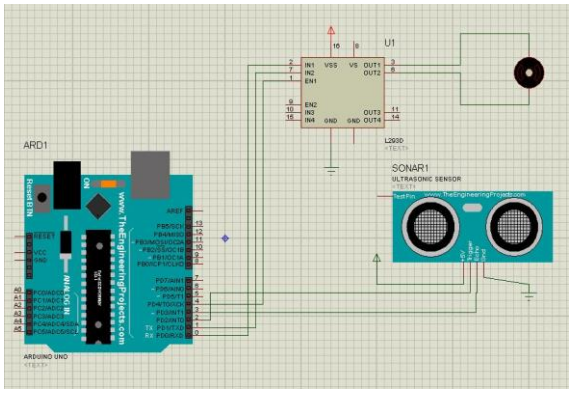

Fig.11. Interfacing diagram of Arduino Uno microcontroller with pump and ultrasonic level sensor

IV. Fabrication and Assembly of Prototype

The required fabrication processes, viz. laser cutting, grinding and drilling were identified and implemented as per the design requirements. Next, joining of the various parts as well as the placement of the ribs over the spars was accomplished initially by using instant adhesive and subsequently by using a permanent adhesive in order to strengthen the bond. In order to ensure proper alignment of the ribs over the load-bearing spars, rectangular wooden alignment spars were used in the wing assembly.

Fig.12. Aileron attached to the wing by 'pivot and round' hinges

Once the ribs were properly joined to the spars in their required positions, the control surfaces were cut manually as per the required dimensions and attached to the wing by using a 5 mm thick balsa sheet and 'pivot and round' hinges. Further, the leading edge, trailing edge, the control surfaces as well as the central part of the wing were masked with a 1 mm thick balsa sheet. To ensure smooth surfaces of the wing, it was covered using a heat shrinkable adhesive covering film.

For the horizontal and the vertical tail, a process similar to that of the wing was adopted. For the fuselage, 1 mm thick balsa sheets were used to cover the top. Velcro was attached to these 1 mm thick balsa sheets as well as the fuselage in order to facilitate easy attachment and removal of the cover for accessing the various electronics housed in the fuselage. A hinge-operated opening was provided in the nose of the fuselage in order to facilitate hassle-free placement of the battery and the ESC in that section of the fuselage as well as to aid the tightening of the motor mount.

Fig.13. Wing masked with 1 mm thick balsa

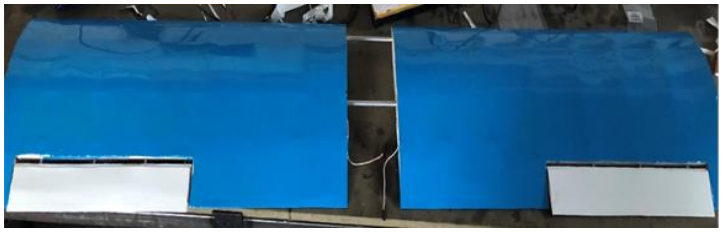

Fig.14. Wing covered with heat shrinkable adhesive covering film

When the fabrication of the individual components of the prototype was completed, the next step was the assembly. The wing was placed in the slots provided in the fuselage and secured using T-nuts and screws. The tail assembly was fastened to the booms using screws, washers and nuts. The booms were then fastened to the fuselage using screws, washers and nuts. The motor mount coupled with the motor and the propeller, the pesticide container and the landing gear were fastened to the fuselage in a similar way. Thus, through the use of fasteners, quick and simple assembly and disassembly of the major components of the prototype was facilitated.

.

Fig.15. Completed UAV Prototype before first test flight

A circular vent was also provided on the side of the pesticide container for easy refuelling of the container without needing to detach it from the fuselage. For ensuring the quick refilling of the pesticide container, a submersible pump identical to the one used in the container was provided along with a pipe.

V. TESTING OF THE PROTOTYPE

Before taking the first test flight, all the individual systems of the UAV needed to be tested separately in order to understand whether the UAV was ready to fly. The first step in the testing of the prototype was to check the control surface responses. The elevator, rudder and the ailerons were tested and found to be working as expected.

Fig.16. Take-off in the first test flight

A mass balancing test was carried out in the longitudinal direction to check whether the obtained Center of Gravity coincided with the theoretical Center of Gravity. It was found that the UAV was pitching upward. To counter this, a small weight was added in the nose of the fuselage.

However, considering the challenges in the dynamic control of the UAV while employing the spraying mechanism, it was decided that the first test flight was to be taken with a dead weight and the spraying mechanism was tested separately, in order to determine whether the pump, spraying head as well the electronics driving the entire spraying system was working as required. It was found that the spraying system was working as per the requirement. The results of both the tests were then used to make the necessary changes in the design.

In the first test flight the UAV flew smoothly and stably and landed safely. The first test flight helped identify the design modifications required which were as follows:

- Initially the tail was designed with a moment arm of 1.0675 m (3.5 ft), considering a value of static margin greater than that required. In the test flight it was found that the UAV flew stably and hence it was proposed to reduce the length of the tail moment arm to 0.915 m (3 ft). The longitudinal dimension of the rudder was doubled, whereas the chord of the elevator was increased by 50% in order to account for the reduction in the length of the tail moment arm.

The change in the length of the tail moment arm will account for the slight imbalance in the Center of Gravity and also obviate the need to add extra weight in the nose to achieve balance. The new configuration was analysed again in XFLR5 and it was found that the Cm vs α graph of the new configuration had a negative gradient, implying static stability.

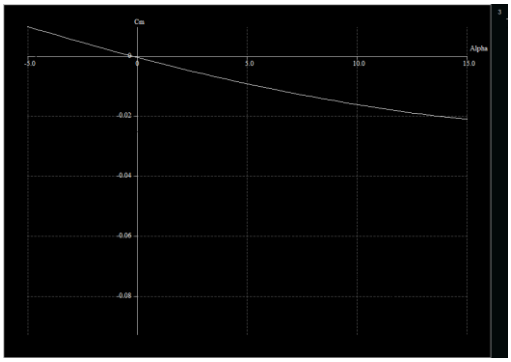

Fig.17. C_m vs α graph for modified horizontal tail

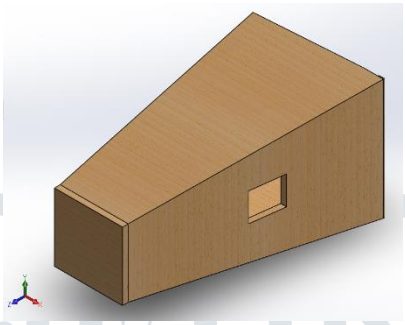

Fig.18. Window/slot in the nose

- It was observed that some arrangement was required for the cooling of the ESC. It was proposed to make small slots/windows in the nose of the fuselage to facilitate the cooling of the ESC. Fig.18 shows the proposed slots in the nose.
- It was proposed to use Z-bent control rods instead of the ones originally used in order to strengthen the integrity of the joints connecting the control rods and the servomotors.

Fig.19. Cruising in the first test flight

After the aforementioned design changes are made, the second flight test will be conducted deploying the spraying system.

ACKNOWLEDGMENT

We would like to express our gratitude to Dr. Jayesh L. Minase for his guidance and support, as well as the Department of Mechanical Engineering, Sinhgad College of Engineering for providing the facilities required to execute the fabrication process. In addition, we would like to thank our colleagues for their direct and indirect help during the project.

REFERENCES

[1] www.theuav.com

[2] D. Giles and R. Billing, "Deployment and performance of a UAV for crop spraying," Chemical Engineering Transactions, Vol. 44, 2015, pp. 307-312.

[3] G.D Goh, S. Agarwala, G.L. Goh, V. Dikshit, W.Y. Yeong, "Additive manufacturing in unmanned aerial vehicles (UAVs): Challenges and potential," Aerospace Science and Technology Vol. 63, April 2017, pp. 140-151

[4] P.K. Freeman and R.S. Freeland, "Agricultural UAVs in the US: potential, policy and hype," Remote Sensing Applications: Society and Environment, Vol. 2, December 2015, pp. 35-43.

[5] G.M. Calvert, L.N. Mehler, J. Alsop, A.L. De Vries, N. Besbelli, "Surveillance of pesticide-related illness and injury in humans," Hayes Handbook of Pesticide Toxicology, 3rd edition, Academic Press, 2010, pp. 1313-1369.

[6] S.G. Kontogiannis, J.A. Ekaterinaris, "Design, performance evaluation and optimization of a UAV," Aerospace Science and Technology, Vol. 29, Issue 1 August 2013, pp. 339-350.

[7] P. Panagiotou, P. Kaparos, C. Salpingidou, K. Yakinthos, "Aerodynamic Design of a MALE UAV," Aerospace Science and Technology, Vol. 50, March 2016, pp. 127-138.

[8] Y. Huang, S.J. Thomson, W.C. Hoffmann, Y. Lan, B.K. Fritz, "Development and prospect of unmanned aerial vehicle technologies for agricultural production management," International Journal of Agricultural and Biological Engineering, Vol. 6, September 2013, pp. 1-10.

[9] E.A. Ahmed, A. Hafiz, A.N. Ouda, H.E.H. Ahmed, H.M. Abd-Elkander, "Modelling of a Small Unmanned Aerial Vehicle," Advances in Robotics and Automation, Vol. 4, Issue 1, January 2015.

[10] F. Cappello, S. Ramasamy, R. Sabatini, "A low-cost and high-performance navigation system for small RPAS applications," Aerospace Science and Technology, Vol. 58, November 2016, pp. 529-545

[11] D.P. Raymer, Aircraft Design: A Conceptual Approach, American Institute of Aeronautics and Astronautics, Reston, VA, 1992.

[12] J.D. Anderson, Aircraft Performance and Design, WCB/McGraw-Hill, Boston, Mass., 1999.

[13] http://www.fao.org /docrep/003/x6897e/x6897e06.html

[14] M.H. Sadraey, Aircraft Design: A Systems Engineering Approach, John Wiley & Sons, Ltd., 2013.

[15] S. Gudmundsson, General Aviation Aircraft Design: Applied Methods and Procedures, Elsevier Inc., 2014